Organic & Biomolecular Chemistry

www.rsc.org/obc

Volume 10 | Number 22 | 14 June 2012 | Pages 4301–4472

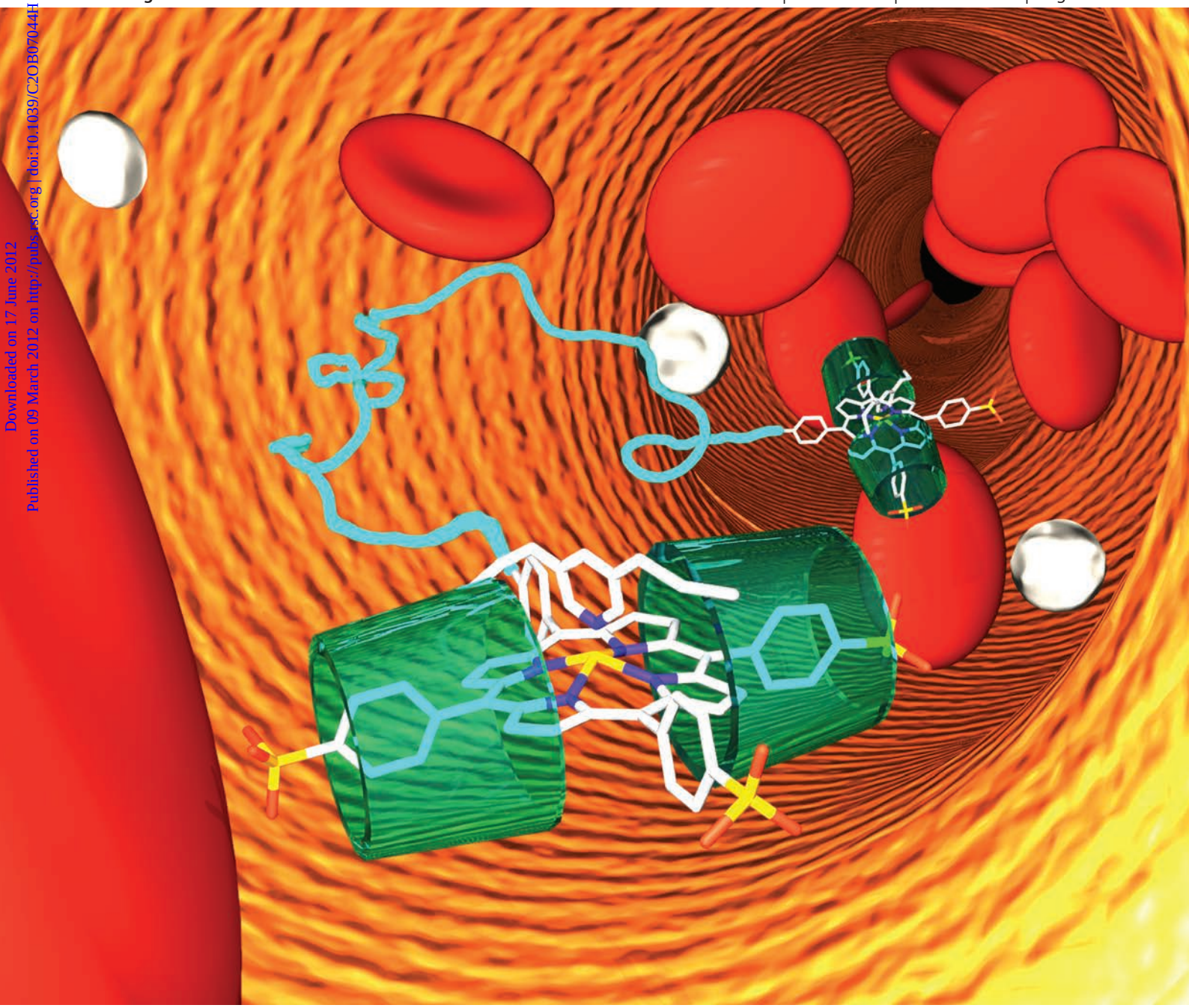

ISSN 1477-0520

RSC Publishing

FULL PAPER

Koji Kano *et al.*

PEGylation of an artificial O_2 and CO receptor: synthesis, characterisation and pharmacokinetic study

1477-0520(2012)10:22;1-F

Organic & Biomolecular Chemistry

Dynamic Article Links
View Online

Cite this: *Org. Biomol. Chem.*, 2012, **10**, 4337

www.rsc.org/obc

PAPER

PEGylation of an artificial O_2 and CO receptor: synthesis, characterisation and pharmacokinetic study†

Takunori Ueda, Hiroaki Kitagishi and Koji Kano*

Received 7th December 2011, Accepted 8th March 2012
DOI: 10.1039/c2ob07044h

A synthetic oxygen (O_2) and carbon monoxide (CO) receptor (hemoCD) composed of 5,10,15,20-tetrakis-(4-sulfonatophenyl)porphinatoiron(II) and a per-*O*-methylated β-cyclodextrin dimer with a pyridine linker (Py3CD) was functionalised with poly(ethylene glycol) (PEG) to elongate the circulation time of the receptor in the bloodstream. α-PEG monocarboxylic acid ($HOOC(CH_2)_3(CO)O$-PEG(mw)-OCH_3; mw = 750 or 5k) or α,ω-PEG dicarboxylic acid ($HOOC(CH_2)_3(CO)O$-PEG(mw)-$O(CO)(CH_2)_3COOH$; mw = 10k or 20k) was reacted with the amino group of 5-(4-aminophenyl)-10,15,20-tris(4-sulfonatophenyl)porphyrin to afford a porphyrin monomer having a PEG chain or a porphyrin dimer having a PEG linker, respectively. The ferrous complexes of these PEGylated porphyrins (PEG750-, PEG5k-, PEG10k- and PEG20k-hemoCDs) bound O_2 in aqueous solution, $P_{1/2}$ values being 6.5–8.1 Torr at pH 7.0 and 25 °C. Each PEG(mw)-hemoCD was infused into the femoral vein of a Wistar male rat. After 6 h of the infusions, 67, 82, 86 and 42% of PEG750-, PEG5k-, PEG10k- and PEG20k-hemoCD were excreted in the urine. PEG750-hemoCD with a hydrodynamic diameter (D_h) of 3.4 nm seemed to partly leak from the blood vessels (pore size: 2–6 nm) before renal filtration (pore size: 4–14 nm). PEG5k- (D_h = 6.2 nm) and PEG10k-hemoCDs (9.0 nm) hardly passed through the blood vessels but were fully filtered by the kidney, resulting in high excretion rates. A considerable amount of PEG20k-hemoCD (D_h = 12.0 nm) was retained in the blood even at 6 h after administration. The present study demonstrates that the behaviour of hemoCD in blood after administration can be controlled by modification of hemoCD with PEG having an appropriate molecular weight.

Introduction

Artificial dioxygen (O_2) carriers have been extensively studied in the development of blood substitutes that can be tentatively used without having to consider the blood type or the risk of infectious diseases.[1–5] Cell-free haemoglobin (Hb) has the ability to reversibly bind dioxygen under physiological conditions. However, Hb itself is not appropriate for use as a blood substitute because of its very short circulation time in the bloodstream (0.5–1.5 h).[5,6] Hb injected into the bloodstream rapidly dissociates from the $\alpha_2\beta_2$ tetramer into the αβ dimer, which is easily eliminated by renal clearance and extravascular leakage due to its small molecular size (the αβ dimer is *ca*. 4 nm in diameter) in comparison to that of red blood cells (7–8 μm in diameter). Hb diffused into the interstitial space causes vasoconstriction and hypertension because of its binding with endogenous nitric oxide (NO)[7,8] and/or the oversupply of dioxygen to the tissue, which induces a reduction in the blood flow.[9,10] A number of chemically modified Hbs, such as oligomerised and polymer-conjugated Hbs, have been prepared to retain Hb in the bloodstream.[11–13] Hb-vesicles containing highly concentrated Hb in the cores of phospholipid vesicles are effective at retaining Hb in the blood.[4,14,15] These artificial dioxygen carriers are called Hb-based oxygen carriers (HBOCs) and show longer circulation times with low toxicities.

A serious problem with HBOCs is the source of the Hb. Hb from human or bovine blood has been utilised for preparation of HBOC.[2,3,16] Hb from such sources might be conceived as a carrier of infectious diseases, even if its purification and chemical modification processes mostly eliminate potential pathogens. In addition, there is an ethical problem in the use of naturally sourced Hb. Although recombinant Hb from bacteria can completely eliminate concerns of infection, it is very costly when prepared in large quantities.[2] Therefore, a totally synthetic oxygen carrier is highly preferable. Tsuchida *et al*. embedded a synthetic iron(II)porphyrin (a picket-fence porphyrin originally designed by Collman *et al*.[17,18]) into phospholipid vesicles.[19]

Department of Molecular Chemistry and Biochemistry, Doshisha University, Tatara, Kyotanabe, Kyoto 610-0321, Japan. E-mail: kkano@mail.doshisha.ac.jp; Fax: +81 774 65 6845; Tel: +81 774 65 6624

†Electronic supplementary information (ESI) available. See DOI: 10.1039/c2ob07044h

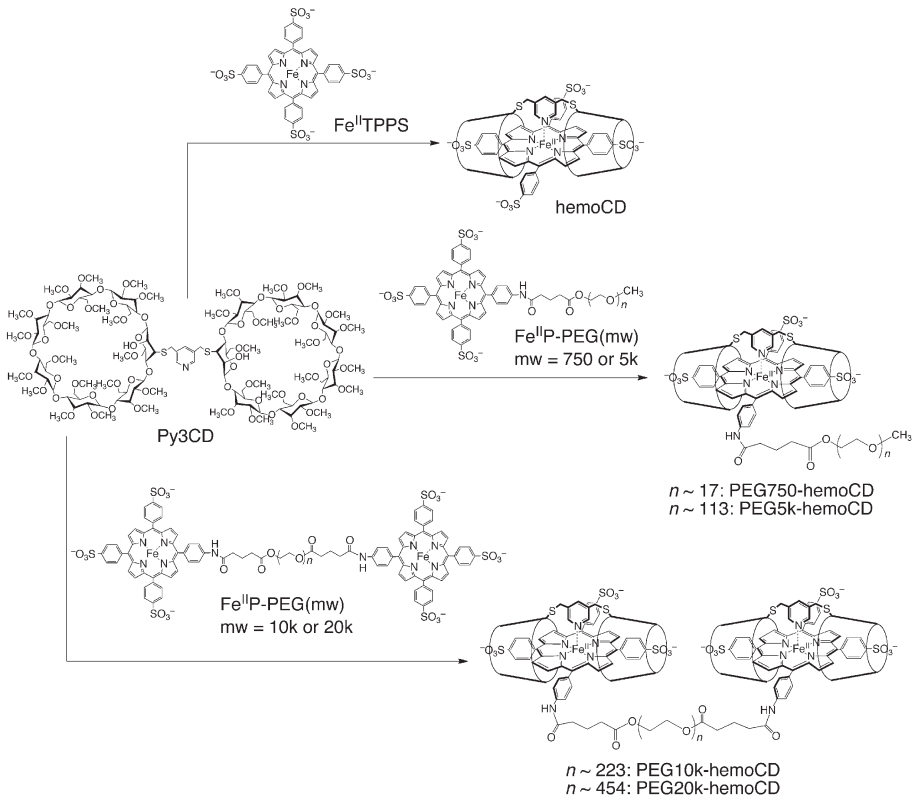

Fig. 1 Structures of hemoCD and PEG(mw)-hemoCDs composed of per-*O*-methylated β-cyclodextrin dimer with a pyridine linker (Py3CD) and iron(II)porphyrins.

It is generally accepted that a dioxygen adduct of an iron(II)-porphyrin in aqueous solution is instantaneously oxidised to an iron(III)porphyrin and a superoxide ion through the nucleophilic attack of a water molecule on the Fe(II)–O_2 bond.[20] A hydrophobic lipid membrane of the vesicle enables the stabilization of the O_2–Fe(II)porphyrin complex by excluding water molecules from an O_2-binding site. The vesicles transport dioxygen in the bloodstream of rabbits and dogs with a circulation half-life of *ca*. 12 h.[21] However, high doses of the vesicles kill the animals because of acute toxicity.[21]

Several years ago, we prepared a totally artificial dioxygen receptor, hemoCD, that functions in aqueous solution.[22,23] HemoCD is a supramolecular 1 : 1 inclusion complex of 5,10,15,20-tetrakis(4-sulfonatophenyl)porphinatoiron(II) (Fe^{II}-TPPS) with a per-*O*-methylated β-cyclodextrin dimer having a pyridine linker (Py3CD) (Fig. 1). The encapsulation of Fe^{II}TPPS by two per-*O*-methylated β-cyclodextrin units provides a hydrophobic environment around the Fe^{II}-center[24] and protects the Fe^{II}–O_2 bond from irreversible autoxidation catalysed by H_2O. The dioxygen and carbon monoxide (CO) affinities ($P_{1/2}$) of hemoCD are 10 and 0.000015 Torr, respectively.[23,25] The molecular size of hemoCD (*ca*. 2.8 nm, *vide infra*) is quite small, and therefore, intravenously infused hemoCD is rapidly excreted in the urine in a CO-coordinated form within 30 min.[26] HemoCD binds endogenous CO in the blood. Approximately 70% of the infused hemoCD molecules are finally excreted in the urine, and the remaining 30% seem to diffuse from the bloodstream into interstitial tissue. We attached hemoCD to poly(acrylic acid)[25] and gold nanoparticle[27] platforms in order to lengthen the circulation time of hemoCD in the bloodstream. The circulation times of these materials in the bloodstream have not yet been determined, although no excretion of either of the materials in the urine was observed. Attaching hemoCD to the polymers and the Au-nanoparticles causes the common problem of destabilization of the O_2-adducts of these receptors. We assumed that the destabilization of the O_2-adducts is ascribed to high local-concentration of the hemoCD moieties on these platforms.[25,27]

In the present study, we employed poly(ethylene glycol) (PEG) to regulate the pharmacokinetic behaviour of hemoCD. PEG is often used to modify drugs and proteins because it is a water-soluble and biocompatible polymer.[28,29] Four different PEGs with average molecular weights (mw) of 750, 5000 (5k), 10 000 (10k) and 20 000 (20k) were covalently bound to hemoCD to investigate the effects of molecular size (Fig. 1). The problem of the local concentration of the hemoCD moiety on stabilization of the O_2-adduct may be avoided in the present system. The behaviours of the PEGylated hemoCDs as O_2 receptors were investigated *in vitro* and *in vivo*.

Results and discussion

Synthesis of PEGylated Fe^{III}TPPS

The synthetic routes of PEGylated Fe^{III}TPPSs (Fe^{III}P-PEG(mw)s) are shown in Schemes 1 and 2. The sulfonatophenyl groups of the porphyrin are very important in preparing a very stable inclusion complex with Py3CD.[23] First, we prepared NH_2-TPPS

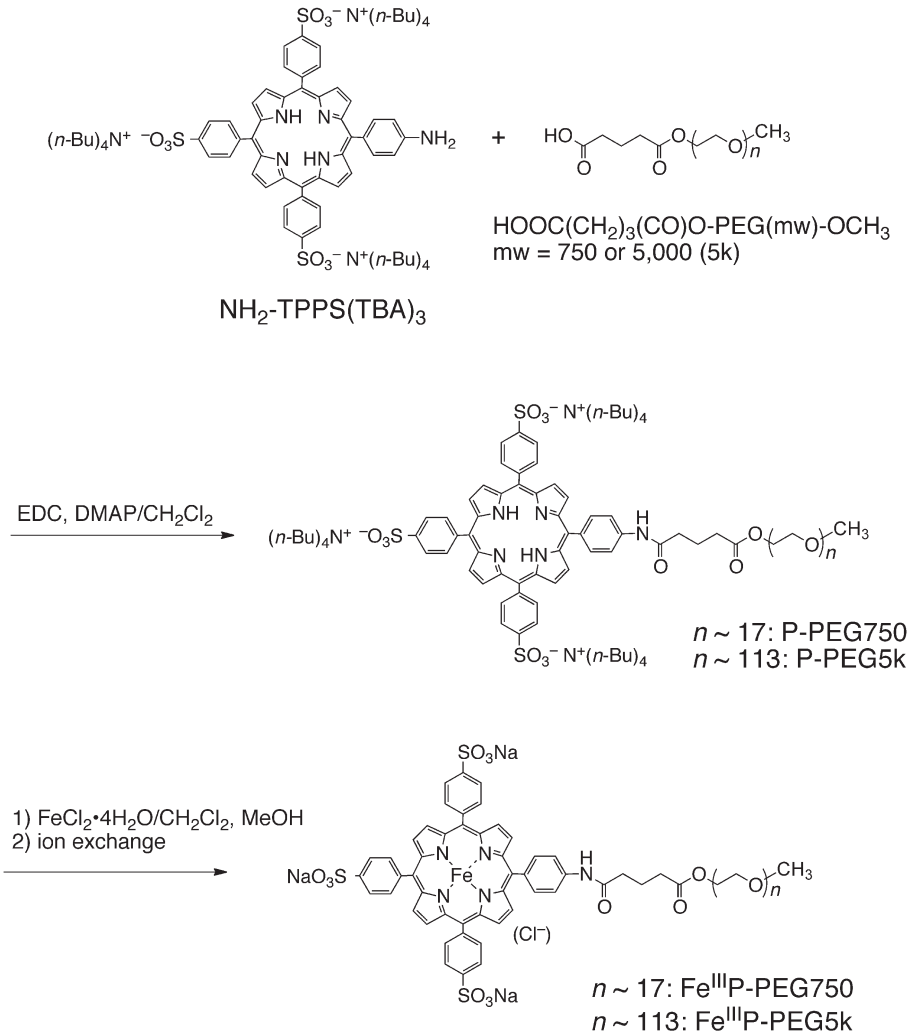

Scheme 1 Synthesis of Fe^{III}P-PEG750 and Fe^{III}P-PEG5k.

$(TBA)_3$,[30,31] which was soluble in dichloromethane. α-PEG carboxylic acid ($HOOC(CH_2)_3(CO)O$-PEG(mw)-OCH_3, mw = 750 or 5k) was condensed with NH_2-TPPS$(TBA)_3$ in dichloromethane in the presence of 1-ethyl-3-(3-dimethylaminopropyl)-carbodiimide (EDC) as a condensation agent to afford the PEGylated porphyrin free bases, P-PEG750 and P-PEG5k (Scheme 1). Because we could not obtain α-PEG carboxylic acids with average molecular weights of 10k and 20k, we used α,ω-PEG dicarboxylic acids ($HOOC(CH_2)_3(CO)O$-PEG(mw)-O-$(CO)(CH_2)_3COOH$; mw = 10k and 20k), which were synthesised from commercial sources.[32] Therefore, both the ends of each higher-molecular-weight PEG dicarboxylic acid were condensed with NH_2-TPPS$(TBA)_3$ to afford a porphyrin dimer with a PEG linker, P-PEG10k or P-PEG20k (Scheme 2). Metallation with $FeCl_2$ gave a series of the ferric complexes of the PEGylated porphyrins (Fe^{III}P-PEG750, Fe^{III}P-PEG5k, Fe^{III}P-PEG10k and Fe^{III}P-PEG20k). These iron porphyrins were characterised by UV-Vis and MALDI-TOF MS spectroscopy (Fig. 2 and Fig. S1–3, ESI†). The UV-Vis spectral shapes of Fe^{III}P-PEG-(mw)s were almost the same as that of Fe^{III}TPPS under the same conditions. We assumed the extinction coefficient of Fe^{III}P-PEG-(mw) at a given wavelength as identical to that of Fe^{III}TPPS.[33] Therefore, the concentration of the porphinatoiron unit could be estimated independently of the molecular weight distribution of PEG.

Complexation of PEGylated Fe^{III}TPPSs with Py3CD

PEGylated ferric hemoCD (PEG(mw)-met-hemoCD) was prepared by including a tris(4-sulfonatophenyl)porphinatoiron(III) moiety attached to the end of a PEG chain with Py3CD (PEG750-met-hemoCD and PEG5k-met-hemoCD), or by including two tris(4-sulfonatophenyl)porphinatoiron(III) moieties attached to both the ends of a PEG chain with Py3CD (PEG10k-met-hemoCD and PEG20k-met-hemoCD) (Fig. 1). Complexation of Fe^{III}P-PEG(mw)s with Py3CD was studied by UV-Vis titration experiments. The spectral changes of Fe^{III}P-PEG5k in 0.05 M phosphate buffer at pH 7.0 on addition of Py3CD are shown in Fig. 3 as an example. The initial spectrum of Fe^{III}P-PEG5k, which corresponds to that of the μ-oxo dimer of Fe^{III}TPPS,[33–35] was regularly changed on addition of Py3CD with three isosbestic points. The final spectrum was quite similar to that of the Fe^{III}TPPS–Py3CD complex with the axial hydroxo

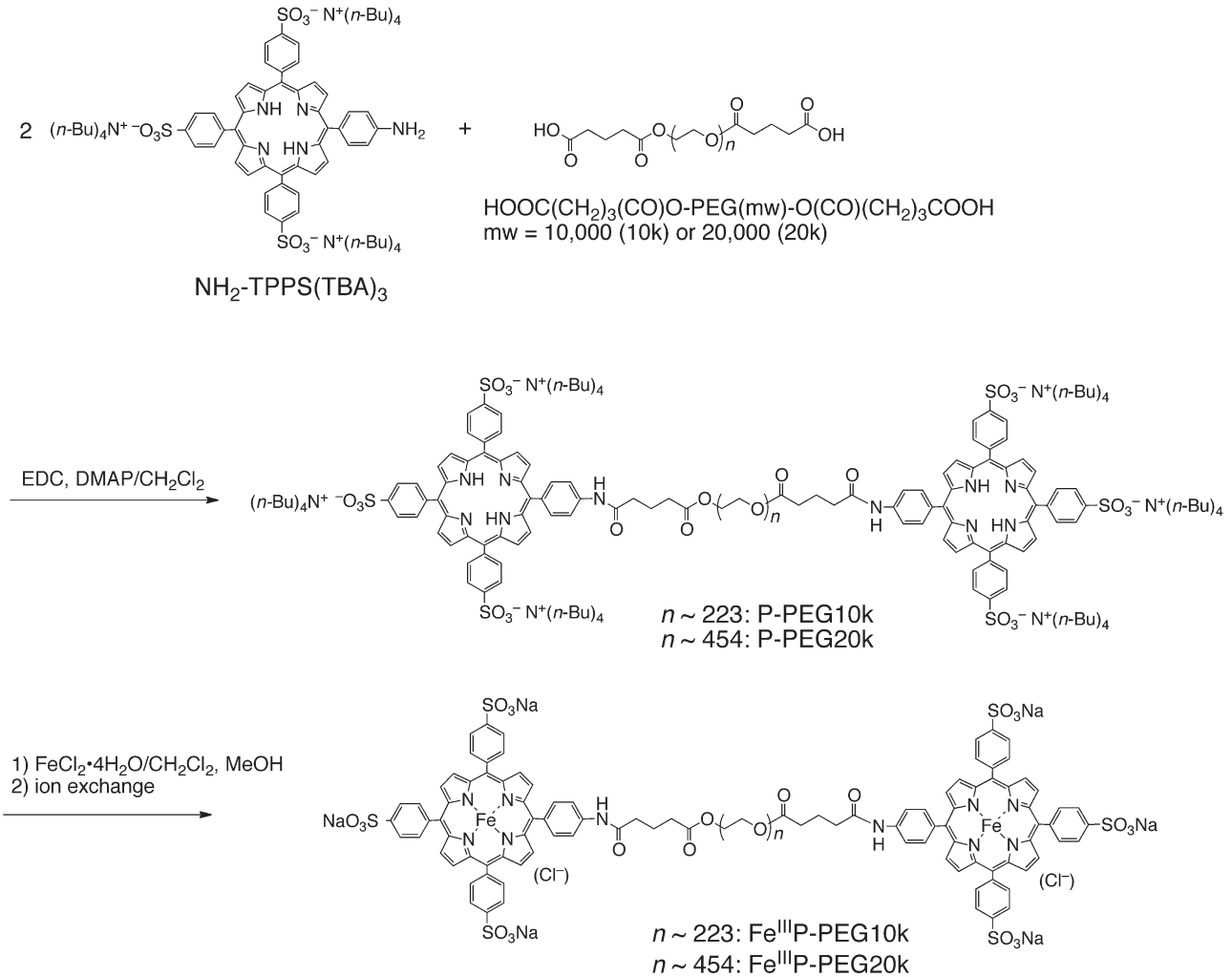

Scheme 2 Synthesis of Fe^{III}P-PEG10k and Fe^{III}P-PEG20k.

and pyridine ligands (met-hemoCD),[22,35] indicating the inclusion of the porphinatoiron(III) unit in Fe^{III}P-PEG5k with Py3CD. The titration curves followed at different wavelengths (Fig. 3 inset) fit well with an equation for a 1 : 1 complexation model to give a binding constant (K). Spectral changes similar to Fig. 3 were measured in the cases of Fe^{III}P-PEG750, Fe^{III}P-PEG10k and Fe^{III}P-PEG20k (Fig. S4–6, ESI†), and the K values for complexation of Fe^{III}P-PEG(mw)s with Py3CD obtained from the spectral titrations are summarised in Table 1. We previously reported that the K value for the Fe^{III}TPPS–Py3CD system is too large to be determined by the UV-Vis titration experiment.[22] However, as given by Table 1, all Fe^{III}P-PEGs with PEG chains show smaller K values. The K value decreases with the increasing chain length of PEG. The interactions between Fe^{III}P-PEG(mw)s and Py3CD were also studied by isothermal titration calorimetry (ITC). Large exothermic peaks were measured on addition of Py3CD to the solutions of Fe^{III}P-PEG(mw)s (Fig. S7, ESI†). The heat changes upon complexation could be analysed based on the 1 : 1 complexation of Py3CD with the porphyrin unit of Fe^{III}P-PEG(mw)s to give K values and thermodynamic parameters (Table 1). The K values determined from ITC are in good agreement with those from the UV-Vis titrations. The decrease in K value with increasing chain length of PEG is attributed to the decrease in the entropy change (ΔS^0). The most plausible explanation for the decrease in ΔS^0 is that the mobility of a PEG chain is partly restricted upon complexation of Fe^{III}P-PEG(mw) with Py3CD because of molecular interactions between the PEG chain and the porphyrin–Py3CD complex in PEG(mw)-met-hemoCD. Such molecular interactions seem to increase with the increasing chain length of PEG. In view of these facts, 1.5 equiv. of Py3CD was added to a Fe^{III}P-PEG(mw) solution in the following experiments to achieve complete inclusion of the porphyrin chromophore with Py3CD.

Dioxygen binding of PEG(mw)-hemoCDs

Ferrous PEG(mw)-hemoCD (PEG(mw)-hemoCD) was prepared by adding $Na_2S_2O_4$ to a mixture of Fe^{III}P-PEG(mw) and Py3CD (1.5 equiv. to the porphyrin unit) in 0.05 M phosphate buffer at pH 7.0. Excess $Na_2S_2O_4$ and its oxidised derivatives were removed by a Sephadex G-25 desalting column. The UV-Vis spectrum of the eluate indicated that each PEG(mw)-hemoCD captured dioxygen during this treatment under aerobic conditions

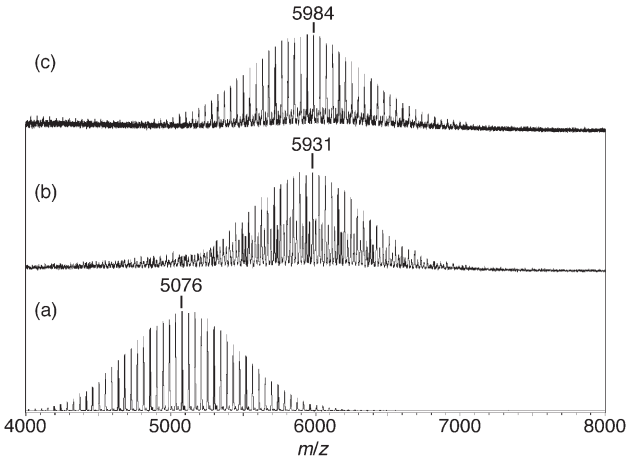

Fig. 2 MALDI-TOF MS spectra of $HOOC(CH_2)_3(CO)O$-PEG5k-OCH_3 (a, positive mode), P-PEG5k (b, negative mode), and Fe^{III}P-PEG5k (c, negative mode) with the subsequent addition of a matrix composed of α-cyano-4-hydroxycinnamic acid and 2,5-dihydroxybenzoic acid. The theoretical mass differences between $HOOC(CH_2)_3(CO)$-O-PEG5k-OCH_3 (a) and P-PEG5k (b) and between P-PEG5k (b) and Fe^{III}P-PEG5k-OMe (c) are 849 and 56, respectively.

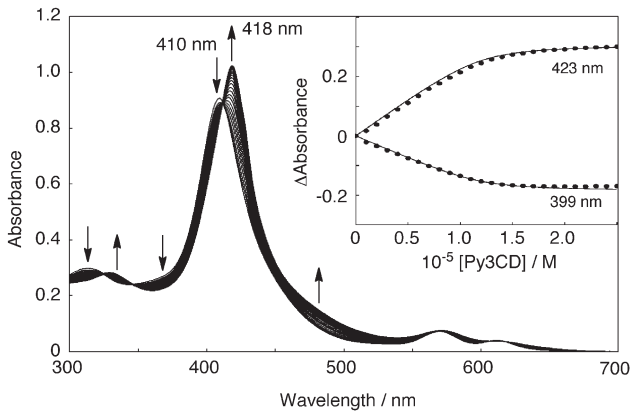

Fig. 3 UV-Vis spectral changes of Fe^{III}P-PEG5k (1×10^{-5} M) on addition of Py3CD in 0.05 M phosphate buffer at pH 7.0 and 25 °C. The inset shows plots of the changes in absorbances of Fe^{III}P-PEG5k *versus* [Py3CD]. The solid lines indicate the theoretical curves for the 1 : 1 complexation to give the binding constant (*K*).

(*vide infra*). The stock solution of the oxygenated PEG5k-hemoCD was diluted with N_2-saturated 0.05 M phosphate buffer, and then, N_2 gas was bubbled into the solution for 2 min. The UV-Vis spectrum of the sample thus obtained showed a Soret band at 433 nm (spectrum (a) in Fig. 4), which corresponds to the deoxy form of PEG5k-hemoCD.[22] The Soret band at 433 nm shifted to 422 nm upon introducing O_2 into the deoxy PEG5k-hemoCD solution (spectrum (b) in Fig. 4). The species showing λ_{max} at 422 nm was ascribed to dioxygen-coordinated PEG5k-hemoCD (oxy-PEG5k-hemoCD), which could be confirmed by replacing an atmosphere from O_2 to CO. The absorption band at 422 nm was characteristically sharpened and enhanced (spectrum (c) in Fig. 4) on the introduction of CO gas

Table 1 Binding constants and thermodynamic parameters for the complexation of PEGylated Fe^{III}TPPSs (Fe^{III}P-PEG(mw)s) with Py3CD in 0.05 M phosphate buffer at pH 7.0 and 25 °C[a]

	K/M^{-1}		ΔH^0/kJ	ΔS^0/J
	UV-Vis	ITC	mol^{-1}	mol^{-1} K^{-1}
Fe^{III}P-PEG750	2.0×10^7	2.7×10^7	−83	−135
Fe^{III}P-PEG5k	2.1×10^6	2.8×10^6	−90	−178
Fe^{III}P-PEG10k[b]	5.5×10^5	7.6×10^5	−92	−196
Fe^{III}P-PEG20k[b]	1.8×10^5	2.0×10^5	−93	−208

[a] Errors were within 10%. [b] The parameters were calculated based on 1 : 1 complexation of the porphyrin unit with Py3CD.

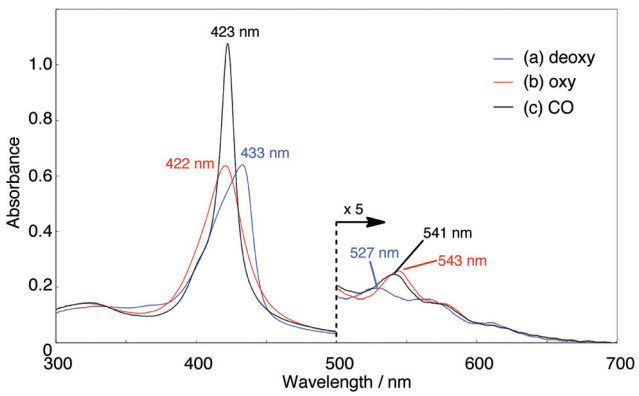

Fig. 4 UV-Vis spectra of PEG5k-hemoCD ([Fe^{II}P-PEG5k] = 3×10^{-6} M, [Py3CD] = 4.5×10^{-6} M) in the deoxy (a, blue), oxy (b, red) and CO-bound forms (c, black) in 0.05 M phosphate buffer at pH 7.0 and 25 °C.

into the solution for 1 min, indicating the formation of CO-coordinated ferrous PEG5k-hemoCD. Essentially the same spectroscopic behaviours were observed for other PEG(mw)-hemoCDs, such as PEG750-hemoCD, PEG10k-hemoCD and PEG20k-hemoCD.

The O_2-adducts of PEG(mw)-hemoCDs (oxy-PEG(mw)-hemoCDs) were gradually autoxidised to the corresponding ferric states. When oxy-PEG(mw)-hemoCDs in 0.05 M phosphate buffer were allowed to stand at 25 °C under aerobic conditions, the UV-Vis spectra changed from the oxy-forms to the ferric-forms (Fig. S8–11, ESI†). The half-lives ($t_{1/2}$) of oxy-PEG-(mw)-hemoCDs were obtained from the pseudo-first-order rate constants (k_{obs}, $t_{1/2} = \ln 2/k_{obs}$) and the results are listed in Table 2. The stabilities of oxy-PEG(mw)-hemoCDs ($t_{1/2} \approx$ 24–27 h) were almost comparable to that of oxy-hemoCD itself ($t_{1/2}$ = 30.1 h)[22] under the same conditions, except for oxy-PEG10k-hemoCD. Oxy-PEG10k-hemoCD was considerably unstable. Two hemoCD moieties of PEG10k-hemoCD are connected with a PEG chain resulting in their approach. We previously found that the dioxygen adduct of highly concentrated hemoCD is deactivated relatively fast because of self-catalysed autoxidation, as formulated in eqn (1)–(4).[25] The highly concentrated oxy-hemoCD in water may cause an apparent disproportionation reaction of the hydroperoxy radical (·OOH) to produce hydrogen peroxide (eqn (1)).[25] It has been reported that H_2O_2

Table 2 Half-lives ($t_{1/2}$) for autoxidation of the O_2-adducts and dioxygen affinities ($P_{1/2}$) of hemoCD and PEG(mw)-hemoCDs in 0.05 M phosphate buffer at pH 7.0 and 25 °C

	$t_{1/2}$/h[a,c]	$P_{1/2}$/Torr[b,c]
HemoCD	30.1[d]	10.0[d]
PEG750-hemoCD	23.5 ± 7.5	6.5 ± 0.5
PEG5k-hemoCD	27.2 ± 4.2	8.1 ± 0.6
PEG10k-hemoCD	13.6 ± 3.0 (26.4 ± 5.9)[e]	7.9 ± 0.4
PEG20k-hemoCD	26.6 ± 4.9	7.6 ± 0.6

[a] The $t_{1/2}$ values were determined from $\ln 2/k_{obs}$, where k_{obs} is the pseudo first-order rate constant of the autoxidation reaction (see Fig. S8–11†). [b] The $P_{1/2}$ values were determined by monitoring UV-Vis spectral changes under various O_2 partial pressures (see Fig. S13–16†). [c] The $t_{1/2}$ and $P_{1/2}$ values of PEG(mw)-hemoCDs were obtained from at least three independent experiments. [d] Ref. 22 and 25. [e] The datum in the parenthesis was measured in the presence of catalase (100 units, see Fig. S12†).

promotes autoxidation of the dioxygen adduct of the ferrous porphyrin (eqn (2)–(4)).[20,36]

$$2Fe^{II}\text{–}O_2 + 2H_2O \rightarrow 2Fe^{III}(OH^-) + H_2O_2 + O_2 \quad (1)$$

$$Fe^{II}\text{–}O_2 + H_2O_2 \rightarrow Fe^{IV} + O_2 + 2OH^- \quad (2)$$

$$Fe^{II}\text{–}O_2 + Fe^{IV} \rightarrow 2Fe^{III} + O_2 \quad (3)$$

$$2Fe^{III} + 2OH^- \rightarrow 2Fe^{III}(OH^-) \quad (4)$$

Our previous study revealed that the autoxidation of the oxy-hemoCD unit attached to a poly(acrylic acid) chain proceeds faster than oxy-hemoCD itself because of higher local concentration of the hemoCD unit in the polymer chain. Similar self-catalysed autoxidation of the dioxygen adduct seems to occur in the oxy-PEG10k-hemoCD system. The fact that the half-life of oxy-PEG10k-hemoCD became longer in the presence of catalase (Fig. S12, ESI† and Table 2) supports the occurrence of self-catalysed autoxidation of oxy-PEG10k-hemoCD. It can be concluded that the average local concentration of oxy-PEG10k-hemoCD is higher than those of other oxy-PEG(mw)-hemoCDs. The experimental result suggests that two hemoCD units in an oxy-PEG20k-hemoCD are well separated from each other by a longer PEG chain, resulting in the absence of self-catalysed autoxidation.

The dioxygen affinity of an O_2-receptor is evaluated by $P_{1/2}$, which corresponds to the partial O_2 pressure (P^{O2}) at which half of the receptor molecules are oxygenated. The $P_{1/2}$ values of PEG(mw)-hemoCDs were determined by monitoring the changes in the absorbances (ΔA) of ferrous PEG(mw)-hemoCDs under various O_2 partial pressures (P^{O2}) (Fig. S13–16, ESI†). $P_{1/2}$ is correlated with P^{O2} by the following equation;[23]

$$P^{O2} = (\Delta\varepsilon\,[\text{PEG(mw)} - \text{hemoCD}]_t\, P^{O2})/\Delta A - P_{1/2} \quad (5)$$

where $\Delta\varepsilon$ is the difference in the extinction coefficients between the deoxy- and oxy-forms at a given wavelength. The linear regression for the plot between $P^{O2}/\Delta A$ and P^{O2} affords a $P_{1/2}$ value. The $P_{1/2}$ values of PEG(mw)-hemoCDs thus determined are listed in Table 2. The $P_{1/2}$ values ranged from 6 to 8 Torr, which were similar to, but slightly smaller than, that of hemoCD (10 Torr).[25] The O_2-affinity of PEG(mw)-hemoCD is independent of the size of the PEG chains.

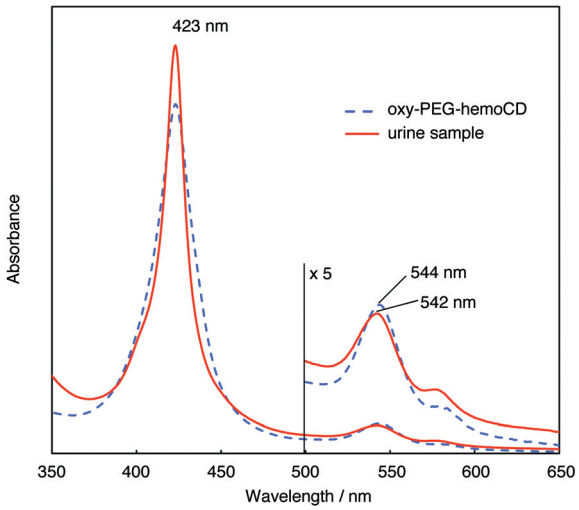

Fig. 5 UV-Vis spectra of a solution of oxy-PEG20k-hemoCD (5×10^{-6} M) in PBS at 25 °C and the rat's urine collected at 180 min after initiation of the oxy-PEG20k-hemoCD infusion. The urine sample was appropriately diluted with PBS.

Pharmacokinetic study

A series of oxy-PEG(mw)-hemoCDs were administered into the femoral veins of rats to determine the effects of a PEG chain on the circulation time in an animal body. The freshly prepared oxy-PEG(mw)-hemoCD solution (0.5 mM as the porphyrin unit) in phosphate buffer saline (PBS) was infused into the femoral vein of a Wistar male rat at a rate of 1 mL h^{-1} for 2 h. Urine was collected at 30 min intervals after initiation of the oxy-PEG(mw)-hemoCD infusion. The urine sample was centrifuged using a conventional centrifuge and the supernatant was appropriately diluted with PBS for measuring a UV-Vis spectrum. Fig. 5 shows an example of the UV-Vis spectrum of a urine sample collected at 180 min after initiation of the oxy-PEG20k-hemoCD infusion. The urine showed a sharp Soret band at 422 nm, suggesting that the urine sample involved CO-coordinated PEG20k-hemoCD. We previously found that administered oxy-hemoCD is rapidly excreted in the urine as a form of the CO-adduct.[26] HemoCD can bind endogenous CO in the rat's body because the CO affinity of hemoCD is approximately 100 times higher than that of human Hb in an R state.[18,23,37] Introducing the CO gas into the urine sample of PEG20k-hemoCD caused an increase in the absorbance at 422 nm due to the conversion of residual oxy-PEG20k-hemoCD to its CO-coordinated form (spectrum (b) in Fig. 6). Subsequent addition of excess $Na_2S_2O_4$ provided further enhancement of the absorption band due to CO-PEG20k-hemoCD (spectrum (c) in Fig. 6), indicating that the urine also includes PEG20k-met-hemoCD. From the spectrum of the urine sample measured in the presence of $Na_2S_2O_4$ under a CO atmosphere, the total amount of PEG20k-hemoCD excreted in the urine (M_{hemoCD}, mol) could be estimated using eqn (6).[26]

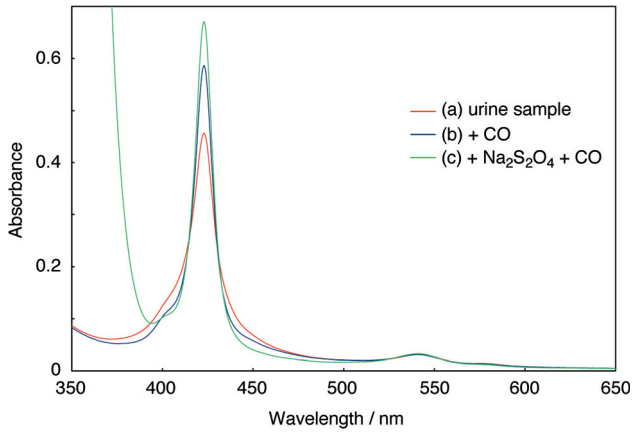

Fig. 6 UV-Vis spectra of the rat's urine collected at 180 min after initiation of the oxy-PEG20k-hemoCD infusion before (a) and after additions of CO (b) and CO/excess $Na_2S_2O_4$ (c) in PBS at 25 °C.

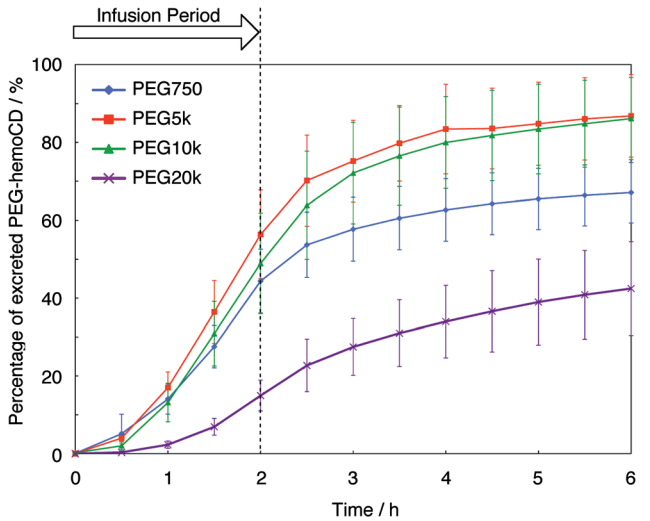

Fig. 7 Timelines of urinary excretion during and after the infusion of oxy-PEG(mw)-hemoCDs (5×10^{-4} M solution in PBS was infused at the rate of 1.0 mL h^{-1} for 2 h). The vertical axis shows the accumulative rate of excreted PEG(mw)-hemoCDs. Each point represents the mean ± SD of the data obtained from three or four experiments using different rats. The statistical treatment of the data is shown in Fig. S17, ESI.†

$$M_{\text{hemoCD}} = (A_{422}V)/(\varepsilon_{422}lD) \quad (6)$$

where A_{422}, V (L), ε_{422} (M^{-1} cm^{-1}), l (cm) and D are the absorbance at 422 nm, the urine volume, the extinction coefficient of CO-PEG20k-hemoCD at 422 nm (Table S1, ESI†), the optical length (1.0 cm) and the dilution factor, respectively. The timelines of the accumulated amounts of the excreted PEG(mw)-hemoCDs are shown in Fig. 7. In the previous study, we found that approximately 70% of the hemoCD molecules infused into the rat's body were excreted in the urine at 6 h after the infusion.[26] Another 30% of the hemoCD molecules seemed to diffuse into the interstitial spaces through the pores of the vascular endothelial walls. In the case of PEG750-hemoCD, 67% of the infused molecules were excreted at 6 h after infusion, suggesting that a short PEG chain of PEG750-hemoCD does not

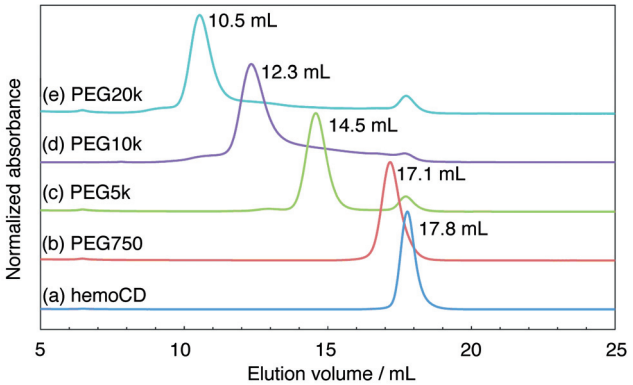

Fig. 8 SEC traces of the ferric-forms of hemoCD and PEG(mw)-hemoCDs. These samples were eluted at a flow rate of 0.5 mL min^{-1} with 0.1 M phosphate buffer at pH 7.0 and 4 °C. Elution was monitored at 408 nm. Absorbance values on the ordinate were normalised to the highest value. The hydrolysed material could be slightly detected at 17.8 mL in traces c, d, and e because PEG(mw)-hemoCD contains a carboxylic ester linkage between PEG and the porphyrin.

have any effect on the pharmacokinetic behaviour. PEG5k- and PEG10k-hemoCDs were excreted more effectively in the urine than hemoCD and PEG750-hemoCD. At 6 h after infusion, 82% and 86% of the PEG5k-hemoCD and PEG10k-hemoCD molecules, respectively, had been excreted. These results suggest that both PEG5k- and PEG10k-hemoCDs hardly pass through the pores of the blood vessels to interstitial spaces, whereas these materials are smoothly filtered by the kidneys. In contrast, only 42% of the infused PEG20k-hemoCD molecules were excreted in the urine, even at 6 h after the infusion, indicating that PEG20k-hemoCD significantly resisted glomerular filtration.

Molecular size is one of the factors determining the circulation time of an administered material in the blood. Therefore, the molecular sizes of PEG(mw)-met-hemoCDs were estimated by size exclusion chromatography (SEC) using a Superdex 200 column. Fig. 8 shows the SEC traces of PEG750-, PEG5k-, PEG10k- and PEG20k-met-hemoCDs. The retention time of PEG(mw)-met-hemoCD shortened as the molecular weight of the PEG chain increased. The hydrodynamic diameters (D_h) of met-hemoCD and PEG(mw)-met-hemoCDs were estimated from a calibration curve prepared using standard proteins (Fig. 9).[38] The hydrodynamic diameters of met-hemoCD and PEG(mw)-met-hemoCDs thus determined are listed in Table 3. The hydrodynamic diameters of met-hemoCD itself and PEG750-met-hemoCD are estimated to be 2.8 and 3.4 nm, respectively. The sizes of the ferrous forms are almost the same as those of the ferric forms. Because the size distributions of the pores of the vascular endothelial wall and the glomerular membrane are 2–6 and 4–14 nm, respectively,[39] both hemoCD and PEG750-hemoCD should easily pass through these pores. Fe^{III}TPPS itself is not excreted in the urine at all because it strongly binds with serum albumin (D_h = 7.1 nm), whereas hemoCD and met-hemoCD do not bind with such a protein.[26] PEG5k- and PEG10k-hemoCDs have hydrodynamic diameters of 6.2 and 9.0 nm, respectively, and may be fully excreted in the urine because their sizes are smaller than those of the pores of the glomerular membrane, even though they rarely pass through the

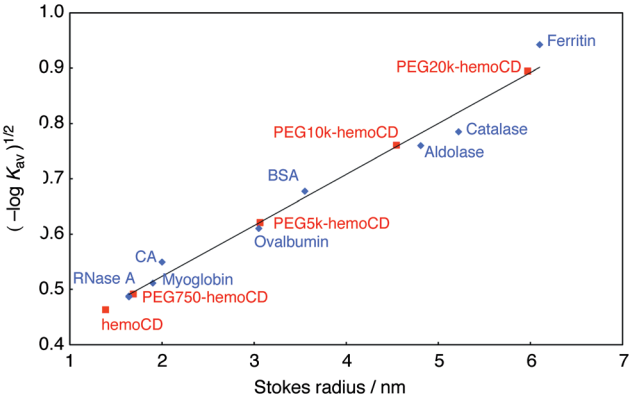

Fig. 9 A calibration curve for estimation of Stokes radii (hydrodynamic radii) of hemoCD and PEG(mw)-hemoCDs (red squares) using standard samples (blue diamonds). Partition coefficients (K_{av}) were determined from the equation $K_{av} = (V_e - V_o)/(V_t - V_o)$, where V_e, V_o and V_t denote the elution volume, the column void volume and the total bed volume of the column, respectively.[38] CA: carbonic anhydrase, RNase A: ribonuclease A, BSA: bovine serum albumin.

Table 3 Hydrodynamic diameters (D_h) of hemoCD and PEG(mw)-hemoCDs

	D_h/nm[a]
HemoCD	2.8
PEG750-hemoCD	3.4
PEG5k-hemoCD	6.2
PEG10k-hemoCD	9.0
PEG20k-hemoCD	12.0

[a] These values were obtained from a calibration curve prepared using standard proteins, shown in Fig. 9.

pores of the vascular endothelial walls. The progressive changes in the SEC traces of the urine after infusion with oxy-PEG5k-hemoCD indicate that PEG5k-hemoCD is excreted in the urine without changes in its molecular size, as shown in Fig. 10. It should be noted that PEG10k-hemoCD (D_h = 9.0 nm) is effectively filtered by the kidney even though its molecular size is larger than that of serum albumin (7.1 nm). In general, a negatively charged material, such as serum albumin (pI ≈ 4.8) and dextran sulfate (6 nm in diameter), resist glomerular filtration.[40] However, anionic PEG10k-hemoCD is smoothly excreted in the urine. Probably, the encapsulation of the sulfonatophenyl groups of the iron(II)porphyrin by two cyclodextrin units of Py3CD reduces electrostatic repulsion between the porphyrin peripherals and the negatively charged glomerular membrane. The rate of excretion of PEG20k-hemoCD (D_h = 12.0 nm) molecules was drastically reduced to 42% at 6 h after the infusion. PEG20k-hemoCD molecules were still leaking from the kidney after 6 h of infusion, suggesting that some PEG20k-hemoCD molecules remained in the bloodstream. To verify this, the serum solution was analysed by SEC and MALDI-TOF MS. The serum sample was prepared by centrifuging the blood sample collected at 6 h after the administration of oxy-PEG20k-hemoCD. Fig. 11a shows the SEC trace of the serum sample. The peak that appeared at 10.5 mL can be attributed to PEG20k-hemoCD (see

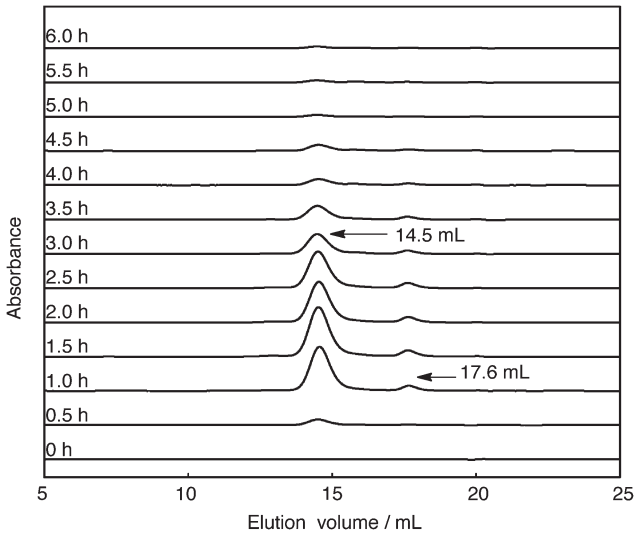

Fig. 10 SEC traces of the urine samples obtained during and after the infusion of oxy-PEG5k-hemoCD (infusion period: initial 2 h). The samples were eluted at a flow rate of 0.5 mL min^{-1} with 0.1 M phosphate buffer at pH 7.0 and 4 °C. Elution was monitored at 408 nm.

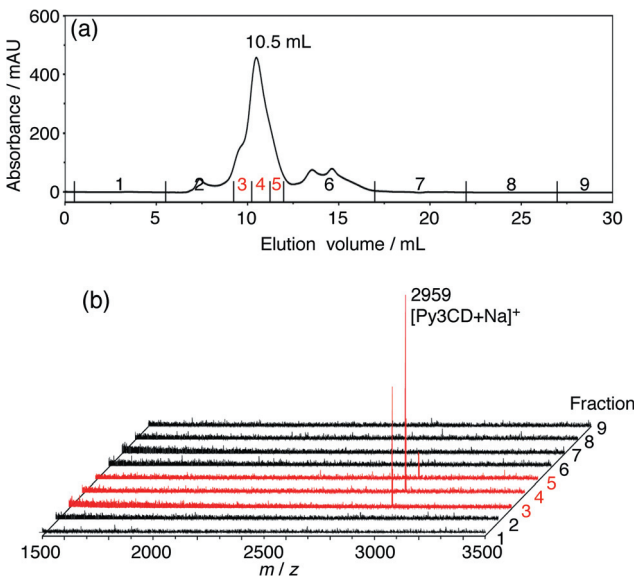

Fig. 11 Analyses of the serum sample collected from the rat's blood at 6 h after the infusion of oxy-PEG20k-hemoCD. (a) A SEC trace of the serum. The sample was eluted at a flow rate of 0.5 mL min^{-1} with 0.1 M phosphate buffer at pH 7.0 and 4 °C. Elution was monitored at 408 nm. The numbers in the chart indicate the fractions. (b) MALDI-TOF MS spectra of the fractionated solutions (positive mode) with subsequent addition of a mixture of α-cyano-4-hydroxycinnamic acid and 2,5-dihydroxybenzoic acid matrices.

Fig. 8e). The eluate from the column was fractionated and each fraction was analysed by MALDI-TOF-MS spectroscopy (Fig. 11b). The peak of m/z = 2959 corresponds to the mass number of [Py3CD + Na]$^+$. The inclusion complex, PEG20k-hemoCD, dissociated to Py3CD and FeP-PEG20k during ionization of the sample. These results indicate that the PEG20k-hemoCD molecules remain in the bloodstream even 6 h after

administration. It can be concluded that the elimination behaviour of hemoCD from the bloodstream can be accurately controlled by changing the length of the PEG chain.

Conclusions

The present study aims to control the circulation time of a hemoCD functive in the bloodstream by attaching PEG chains to the periphery of an iron porphyrin. HemoCD is a multifunctional supramolecule; therefore, PEGylation of hemoCD is expected to expand its usage, allowing it to serve as an artificial dioxygen carrier,[41] a remover of endogenous and exogenous carbon monoxide[26] and a cyanide remover.[42] We prepared four PEG(mw)-hemoCDs, PEG750-, PEG5k-, PEG10k- and PEG20k-hemoCDs, and studied their dioxygen affinities and pharmacokinetic behaviours. The chemical and physiological behaviours of PEG750-hemoCD are almost identical to those of hemoCD. Both hemoCD (D_h = 2.8 nm) and PEG750-hemoCD (3.4 nm) are eliminated through the kidney and the vascular endothelial walls because they have sufficiently small molecular sizes. In contrast, although the molecular sizes of PEG5k- (D_h = 6.2 nm) and PEG10k-hemoCDs (9.0 nm) are suitable for elimination through the kidney, they are unsuitable for elimination through the pores of the vascular endothelial walls. PEG20k-hemoCD (D_h = 12 nm) is gradually excreted in the urine because its size is nearly the maximum size that can be filtered by the renal glomeruli. An iron porphyrin moiety is bound to the PEG chains through a carboxylic ester bond, which may be hydrolysed to the iron porphyrin and PEG fragments in the body. Tetraarylporphinatoiron is strongly bound to Py3CD to retain a 1 : 1 inclusion complex, which is rapidly excreted in the urine. Therefore, synthetic porphinatoiron can be egested completely after it functions as a PEG(mw)-hemoCD. The present study revealed that the circulation time of highly functional hemoCD in the bloodstream can be controlled by introducing a PEG chain.

Experimental section

Instruments

^{1}H NMR spectra were recorded on JEOL JNM-ECA500 and JNM-A400 spectrometers using tetramethylsilane (TMS) as an internal standard. UV-Vis spectra were measured on SHIMADZU UV-2100, UV2450 and MultiSpec-1500 spectrophotometers equipped with thermostatic cell holders. Matrix-assisted laser desorption–ionization time-of-flight mass (MALDI-TOF MS) spectra were recorded on Shimadzu AXIMACFR plus and Bruker Daltonics autoflex speed spectrometers. The mass scale was calibrated by linear regression using 2,3,6-tri-*O*-methyl-β-cyclodextrin (Nacalai, $[M + Na]^+$, m/z = 1451.68, monoisotropic mass) or albumin from bovine serum (Sigma-Aldrich, $[M + H]^+$, m/z = 66 430, average mass). Microcalorimetric measurements were carried out using a MicroCal Isothermal Titration Calorimeter VP-ITC and the data were subsequently analysed using the ORIGIN software program. Size exclusion chromatography (SEC) analyses were performed using a Superdex 200 10/300 GL column (1 × 30 cm) attached to an ÄKTA purifier FPLC system (GE healthcare). Mixed O_2 gases with various partial pressures in N_2 were prepared with a KOFLOC GM-4B gas mixing apparatus.

Materials

Water purified by a MILLIPORE Simpli Lab system was used in all experiments. Pure O_2 (99.998%), N_2 (99.998%) and CO (99.9%) gases were purchased from Sumitomo Seika Chemicals. Phosphate buffer (0.05 M, pH 7.0) and phosphate buffer saline (PBS, 0.05 M phosphate buffer containing 0.9 wt% NaCl at pH 7.4) solutions were prepared using NaH_2PO_4, $NaHPO_4$ and NaCl (Wako). Gel-filtration standard samples with known Stokes radii were purchased from GE Healthcare. Commercially available chemical reagents used for organic syntheses were purchased and used as received. 5-(4-Aminophenyl)-10,15,20-tris(*p*-sulfonatophenyl)porphyrin tetrabutylammonium salt (NH_2-TPPS$(TBA)_3$) was synthesised according to the literature method.[30,31] α-PEG monocarboxylic acid ($HOOC(CH_2)_3(CO)O$-PEG(mw)-OCH_3; mw = 750 and 5k) and α,ω-PEG dicarboxylic acid ($HOOC(CH_2)_3(CO)O$-PEG(mw)-$O(CO)(CH_2)_3COOH$; mw = 10k and 20k) were synthesised from commercially available PEG monomethyl ethers (mw = 750 and 5k, Sigma-Aldrich) and PEGs (mw = 10k, Sigma-Aldrich, and 20k, Wako), respectively, according to the reported method.[32] The synthesis of Py3CD was previously described.[22]

General procedure for conjugating porphyrin with PEG

5-(4-Aminophenyl)-10,15,20-tris(4-sulfonatophenlyl)porphyrin tetrabutylammonium salt (NH_2-TPPS$(TBA)_3$, 0.30–0.64 g) was dissolved in 100–200 mL of dichloromethane. Ten molar equiv. of $HOOC(CH_2)_3(CO)O$-PEG(mw)-OCH_3 or 0.25 molar equiv. of $HOOC(CH_2)_3(CO)O$-PEG(mw)-$O(CO)(CH_2)_3COOH$ was added to the solution, with stirring, at room temperature. 1-Ethyl-3-(3-dimethylaminopropyl)carbodiimide (EDC, 5.0 molar equiv.) and 4-dimethylaminopyridine (DMAP, 5.0 molar equiv.) were then added to the solution. After the mixture was stirred at room temperature for 12 h, the solution was washed with aqueous 5% HCl and saturated $NaHCO_3$ solutions. The organic phase was dried over $Na_2S_2O_4$ and evaporated to dryness to give a purple solid.

P-PEG750. Obtained from the reaction of NH_2-TPPS$(TBA)_3$ (0.50 g, 0.31 mmol) with $HOOC(CH_2)_3(CO)O$-PEG750-OCH_3 (2.6 g, 3.1 mmol). The product was further purified by silica gel column chromatography ($CHCl_3$/MeOH = 10 : 1 to 3 : 1, v/v) to remove excess $HOOC(CH_2)_3(CO)O$-PEG750-OCH_3 and give P-PEG750 as a purple solid (0.56 g, 73%). ^{1}H NMR (400 MHz, $CDCl_3$) δ 8.85–8.70 (m, 8H), 8.31–8.01 (m, 16H), 4.27 (bs, 2H), 3.90–3.50 (m, PEG backbone), 3.37–3.34 (m, 24H), 2.81 (bs, 2H), 2.63 (bs, 2H), 2.21 (bs, 2H), 1.64 (bs, 24H), 1.41 (bs, 24H), 0.96 (bs, 36H), −2.80 (s, 2H); UV-Vis (0.05 M phosphate buffer at pH 7.0) λ_{max}/nm 416, 520, 559, 580 and 639. The MALDI-TOF MS spectrum is shown in Fig. S1, ESI.†

P-PEG5k. Obtained from the reaction of NH_2-TPPS$(TBA)_3$ (0.30 g, 0.18 mmol) with $HOOC(CH_2)_3(CO)O$-PEG5k-OCH_3 (9.1 g, 1.8 mmol). The product was further purified by silica gel column chromatography ($CHCl_3$/MeOH = 10 : 1 to 6 : 1 (v/v)) to

remove excess $HOOC(CH_2)_3(CO)O$-PEG5k-OCH_3 and give P-PEG5k as a purple solid (0.85 g, 72%). ^1H NMR (500 MHz, $CDCl_3$) δ 8.98–8.73 (m, 8H), 8.31–8.04 (m, 16H), 4.35 (bs, 2H), 3.79–3.49 (m, PEG backbone), 3.40–3.37 (m, 24H), 2.72–2.66 (m, 2H), 2.62–2.60 (m, 2H), 2.22–2.20 (m, 2H), 1.75–1.68 (m, 24H), 1.52–1.45 (m, 24H), 1.02 (t, 36H, J = 7.2 Hz), −2.80 (s, 2H); UV-Vis (0.05 M phosphate buffer at pH 7.0) λ_{max}/nm 418, 516, 551, 588 and 644. The MALDI-TOF MS spectrum is shown in Fig. 2b.

P-PEG10k. Obtained from the reaction of NH_2-TPPS$(TBA)_3$ (0.64 g, 0.40 mmol) with $HOOC(CH_2)_3(CO)O$-PEG10k-$O(CO)(CH_2)_3COOH$ (1.0 g, 0.10 mmol) as a purple solid (0.69 g, 53%). The product was used for the next reaction without further purification because the impurities were almost completely removed by the extraction operation described above. ^1H NMR (500 MHz, $CDCl_3$) δ 8.87–8.80 (m, 16H), 8.34–8.07 (m, 32H), 4.35 (bs, 4H), 3.78–3.49 (m, PEG backbone), 3.40–3.36 (m, 48H), 2.69 (t, 4H, J = 6.9 Hz), 2.61 (t, 4H, J = 6.9 Hz), 2.21 (m, 4H), 1.75–1.68 (m, 48H), 1.52–1.45 (m, 48H), 1.04–1.00 (m, 72H), −2.85 (s, 4H); UV-Vis (0.05 M phosphate buffer at pH 7.0) λ_{max}/nm 417, 519, 557, 593 and 650. The MALDI-TOF MS spectrum is shown in Fig. S2, ESI.†

P-PEG20k. Obtained from the reaction of NH_2-TPPS$(TBA)_3$ (0.32 g, 0.20 mmol) with $HOOC(CH_2)_3(CO)O$-PEG(20k)-$O(CO)(CH_2)_3COOH$ (1.0 g, 0.05 mmol) as a purple solid (0.75 g, 65%). The product was used for the next reaction without further purification because the impurities were almost completely removed by the extraction operation described above. ^1H NMR (500 MHz, $CDCl_3$) δ 8.83–8.80 (m, 16H), 8.33–8.01 (m, 32H), 4.37 (s, 4H), 3.79–3.49 (m, PEG backbone), 3.39–3.36 (m, 48H), 2.67 (t, 4H, J = 6.9 Hz), 2.61 (t, 4H, J = 6.9 Hz), 2.24–2.19 (m, 4H), 1.75–1.68 (m, 48H), 1.49 (m, 48H), 1.02 (m, 72H), −2.85 (s, 4H); UV-Vis (0.05 M phosphate buffer at pH 7.0) λ_{max}/nm 418, 518, 554, 591 and 648. The MALDI-TOF MS spectrum is shown in Fig. S3, ESI.†

General procedure for metallation of P-PEG(mw) with $FeCl_2$

A free-base porphyrin bearing a PEG chain (P-PEG(mw), 0.30–0.50 g) was dissolved in 100–150 mL of chloroform and the solution was refluxed for 10 min. To the solution, 20 mL of a saturated $FeCl_2{\cdot}4H_2O$ solution in MeOH was added. The mixture was refluxed for 2 h, and then, the solution was cooled to room temperature and washed with chloroform followed by water. The organic phase was dried over Na_2SO_4 and evaporated to dryness. The residue was dissolved in water and the solution was passed through an ion exchange column (DOWEX MARATHON C, Na^+ form). Water was evaporated from an eluate and the residue was dissolved in the minimum amount of MeOH and purified by gel filtration column chromatography on the Sephadex LH-20 (MeOH). The product was dissolved in the minimum amount of MeOH and reprecipitated by acetone. The purple solid was collected and dried under vacuum to give an iron complex.

Fe^{III}P-PEG750. Obtained from the reaction of P-PEG750 (310 mg, 0.13 mmol) with $FeCl_2{\cdot}4H_2O$ as a dark purple solid (230 mg, 97%). UV-Vis (0.05 M phosphate buffer at pH 7.0) λ_{max}/nm 408, 571 and 612. The MALDI-TOF MS spectrum is shown in Fig. S1, ESI.†

Fe^{III}P-PEG5k. Obtained from the reaction of P-PEG5k (300 mg, 0.046 mmol) with $FeCl_2{\cdot}4H_2O$ as a dark purple solid (185 mg, 54%). UV-Vis (0.05 M phosphate buffer at pH 7.0) λ_{max}/nm 409, 571 and 612. The MALDI-TOF MS spectrum is shown in Fig. 2c.

Fe^{III}P-PEG10k. Obtained from the reaction of P-PEG10k (500 mg, 0.038 mmol) with $FeCl_2{\cdot}4H_2O$ as a dark purple solid (216 mg, 42%). UV-Vis (0.05 M phosphate buffer at pH 7.0) λ_{max}/nm 410, 571 and 613. The MALDI-TOF MS spectrum is shown in Fig. S2, ESI.†

Fe^{III}P-PEG20k. Obtained from the reaction of P-PEG20k (300 mg, 0.013 mol) with $FeCl_2{\cdot}4H_2O$ as a dark purple solid (288 mg, 92%). UV-Vis (0.05 M phosphate buffer at pH 7.0) λ_{max}/nm 410, 571 and 613. The MALDI-TOF MS spectrum is shown in Fig. S3, ESI.†

Animal experiments

Male Wistar rats (SLC, Shizuoka, Japan) weighing 270–350 g were used. The animal experiments were performed in accordance with the Guidelines for Animal Experiments of Doshisha University. The rats were housed three-per-cage under controlled environmental conditions and fed commercial feed pellets. All rats had free access to food and water.

The rats were placed under anesthesia by an intraperitoneal injection of urethane (1.0 g kg^{-1}), and a polyurethane tube (id 0.95 mm, od 1.3 mm) was surgically implanted in their urinary bladders to collect urine samples. The test solution containing oxy-PEG(mw)-hemoCD in PBS was prepared as previously described.[26] The solution was constantly infused into the femoral vein at a rate of 1.0 mL h^{-1} using a variable-speed compact infusion pump, the KDS Model 100 syringe pump (KD Scientific Inc.). Urine was collected at 30 min intervals after initiation of the oxy-PEG(mw)-hemoCD infusion. The bladder was flushed with approximately 1 mL of saline at the end of each urine collection procedure and the effluent was added to the urine collected over that interval.

Acknowledgements

This work was supported by Grants-in-Aid on Scientific Research B (No. 21350097) and "Creating Research Center for Advanced Molecular Biochemistry", Strategic Development of Research Infrastructure for Private Universities from the Ministry of Education, Culture, Sports, Science and Technology.

References

1 J. G. Riess, *Chem. Rev.*, 2001, **101**, 2797–2919.
2 J. E. Squires, *Science*, 2002, **295**, 1002–1005.
3 H. W. Kim and A. G. Greenburg, *Artif. Organs*, 2004, **28**, 813–828.
4 H. Sakai, H. Horinouchi, K. Kobayashi and E. Tsuchida, *J. Int. Med.*, 2008, **263**, 4–15.
5 E. Tsuchida, K. Sou, A. Nakagawa, H. Sakai, T. Komatsu and K. Kobayashi, *Bioconjugate Chem.*, 2009, **20**, 1419–1440.

6 J. P. Savitsky, J. Doczi, J. Black and J. D. Arnold, *Clin. Pharmacol. Ther. (St. Louis)*, 1978, **23**, 73–80.
7 C. D. Reiter, X. Wang, J. E. Tanus-Santos, N. Hogg, R. O. Cannon III, A. N. Schechter and M. T. Gladwin, *Nat. Med.*, 2002, **8**, 1383–1389.
8 B. Yu, M. J. Raher, G. P. Volpato, K. D. Bloch, F. Ichinose and W. M. Zapol, *Circulation*, 2008, **117**, 1982–1990.
9 M. R. McCarthy, K. D. Vandegriff and R. M. Winslow, *Biophys. Chem.*, 2001, **92**, 103–117.
10 R. M. Winslow, *J. Int. Med.*, 2003, **253**, 508–517.
11 S. A. Gould and G. S. Moss, *World J. Surg.*, 1996, **20**, 1200–1207.
12 T. M. S. Chang, *Artif. Organs*, 2004, **28**, 789–794.
13 R. M. Winslow, *Artif. Organs*, 2004, **28**, 800–806.
14 A. S. Rudolph, R. W. Klipper, B. Goins and W. T. Phillips, *Proc. Natl. Acad. Sci. U. S. A.*, 1991, **88**, 10976–10980.
15 K. Sou, R. Klipper, B. Goins, E. Tsuchida and W. T. Phlipps, *J. Pharmacol. Exp. Ther.*, 2005, **312**, 702–709.
16 T. Henkel-Hanke and M. Oleck, *AANA J.*, 2007, **75**, 205–211.
17 J. P. Collman, *Acc. Chem. Res.*, 1977, **10**, 265–272.
18 J. P. Collman, R. Boulatov, C. J. Sunderland and L. Fu, *Chem. Rev.*, 2004, **104**, 561–588.
19 E. Tsuchida, H. Nishide, M. Yuasa, E. Hasegawa and Y.-i. Matsushita, *J. Chem. Soc., Dalton Trans.*, 1984, 1147–1151.
20 K. Shikama, *Chem. Rev.*, 1998, **98**, 1357–1373.
21 K. Kobayashi, E. Tsuchida and H. Nishide, in *Artificial Red Cells*, ed. E. Tsuchida, Wiley, New York, 1995, ch. 5, pp. 93–116.
22 K. Kano, H. Kitagishi, M. Kodera and S. Hirota, *Angew. Chem., Int. Ed.*, 2005, **44**, 435–438.
23 K. Kano, H. Kitagishi, C. Dagallier, M. Kodera, T. Matsuo, T. Hayashi, Y. Hisaeda and S. Hirota, *Inorg. Chem.*, 2006, **45**, 4448–4460.
24 K. Kano, H. Kitagishi, S. Tamura and A. Yamada, *J. Am. Chem. Soc.*, 2004, **126**, 15202–15210.
25 K. Kano, T. Ochi, S. Okunaka, Y. Ota, K. Karasugi, T. Ueda and H. Kitagishi, *Chem.–Asian J.*, 2011, **6**, 2946–2955.
26 H. Kitagishi, S. Negi, A. Kiriyama, A. Honbo, Y. Sugiura, A. T. Kawaguchi and K. Kano, *Angew. Chem., Int. Ed.*, 2010, **49**, 1312–1315.
27 K. Karasugi, H. Kitagishi and K. Kano, *Chem.–Asian J.*, 2011, **6**, 825–833.
28 J. M. Harris, N. E. Martin and M. Modi, *Clin. Pharmacokinet.*, 2001, **40**, 539–551.
29 R. Webster, E. Didier, P. Harris, N. Siegel, J. Stadler, L. Tilbury and D. Smith, *Drug Metab. Dispos.*, 2007, **35**, 9–16.
30 W. J. Kruper Jr., T. A. Chamberlin and M. Kochanny, *J. Org. Chem.*, 1989, **54**, 2753–2756.
31 M. Endo, M. Fujitsuka and T. Majima, *Chem.–Eur. J.*, 2007, **13**, 8660–8666.
32 J. Li and W. J. Kao, *Biomacromolecules*, 2003, **4**, 1055–1067.
33 E. B. Fleischer, J. M. Palmer, T. S. Srivastava and A. Chatterjee, *J. Am. Chem. Soc.*, 1971, **93**, 3162–3167.
34 S. Mosseri, J. C. Mialocq and B. Perly, *J. Phys. Chem.*, 1991, **95**, 4659–4663.
35 K. Kano, S. Chimoto, M. Tamaki, Y. Itoh and H. Kitagishi, *Dalton Trans.*, 2012, **41**, 453–461.
36 K. Yusa and K. Shikama, *Biochemistry*, 1987, **26**, 6684–6688.
37 V. S. Sharma, M. R. Schmidt and H. M. Ranney, *J. Biol. Chem.*, 1976, **251**, 4267–4272.
38 P. Klatt, S. Pfeiffer, B. M. List, D. Lehner, O. Glatter, H. P. Bächinger, E. R. Werner, K. Schmidt and B. Mayer, *J. Biol. Chem.*, 1996, **271**, 7336–7342.
39 M. E. Fox, F. C. Szoka and J. M. J. Fréchet, *Acc. Chem. Res.*, 2009, **42**, 1141–1151.
40 M. P. Bohrer, C. Baylis, H. D. Humes, R. J. Glassock, C. R. Robertson and B. M. Brenner, *J. Clin. Invest.*, 1978, **61**, 72–78.
41 K. Kano and H. Kitagishi, *Artif. Organs*, 2009, **33**, 177–182.
42 K. Watanabe, H. Kitagishi and K. Kano, *ACS Med. Chem. Lett.*, 2011, **2**, 943–947.